is probably due to the interaction of the ether solvent with the lithium cation of the aggregate.

Acknowledgment. This work was supported by NSF Grant CHE-8709249 to E.M.A., for which we are most appreciative. We acknowledge Dr. Anthony A. Ribeiro of the Duke Magnetic Resonance Center for his assistance in the implementation of the ^6Li-^1H NOE NMR experiment and Dr. Franklin J. Fisher for initial thermochemical experiments.

Supplementary Material Available: Atomic numbering scheme and tables of crystallographic data, atomic positional and thermal parameters, bond lengths and angles, and selected torsion angles for lithium (-)-*N*-methylephedrate benzene solvate (14 pages); listing of observed and calculated structure amplitudes (18 pages). Ordering information is given on any current masthead page.

Molecular Recognition of Quinones: Two-Point Hydrogen-Bonding Strategy for the Construction of Face-to-Face Porphyrin-Quinone Architectures[1]

Yasuhiro Aoyama,*[,†,2] Masumi Asakawa,[†] Yuichi Matsui,[†] and Hisanobu Ogoshi*[,‡]

Contribution from the Department of Chemistry, Nagaoka University of Technology, Kamitomioka, Nagaoka, Niigata 940-21, Japan, and Department of Synthetic Chemistry, Kyoto University, Sakyo-Ku, Kyoto 606, Japan. *Received February 18, 1991*

Abstract: 5,15-*cis*-Bis(2-hydroxy-1-naphthyl)octaethylporphyrin (**1**) in chloroform selectively binds *p*-quinones via a two-point hydrogen-bonding interaction between the two, convergent hydroxyl groups of host **1** and the two carbonyl moieties of a guest quinone. Upon complexation, the ^1H NMR resonance and IR absorption for the OH groups undergo a characteristic downfield shift and a shift to lower wavenumber, respectively ($\Delta\delta_{comp}$(OH) = 1.38-2.85 ppm and $\Delta\nu_{comp}$(OH) = 30-102 cm^{-1}, depending on the basicities of quinones). The binding constants (K) evaluated by ^1H NMR titration at 298 K decrease in the order anthraquinone (**17**; 2.3×10^2 M^{-1}) > naphthoquinone (**15**; 1.7×10^2) > benzoquinone (**5**; 5.5×10): Those for benzoquinone derivatives are duroquinone (**12**; 4.2×10^2) > chloranil (**6**; 4.0×10^2) > fluoranil (**7**; 3.7×10^2) > 2,5-dichlorobenzoquinone (**8**; 2.2×10^2) > 2-chlorobenzoquinone (**9**; 1.2×10^2) > 2,5-dimethylbenzoquinone (**11**; 1.1×10^2) > 2-methylbenzoquinone (**10**; 8.8×10) > benzoquinone (**5**; 5.5×10) > 2,3-dimethoxy-5-methylbenzoquinone (**13**; 3.5×10) > tetramethoxybenzoquinone (**14**; 7.8). The variation in K's suggests that the strength of hydrogen bonds, direct porphyrin-quinone interaction apparently of a charge-transfer type, and the steric effects of methoxy substituents are important factors. Reference guests such as anthrone (**18**; K = 4.2 M^{-1}), *o*-naphthoquinone (**16**; 8.7), and 1,4-cyclohexanedione (**19**; 1.0×10) show significantly lower affinities to host **1** than those for the corresponding *p*-quinone counterparts. The resulting **1**-quinone adducts have an estimated face-to-face separation of as short as 3 Å and exhibit porphyrin-quinone π-π interaction as revealed by UV/visible spectroscopy; the longest wavelength absorption band of **1** undergoes either a blue shift or a red shift depending on the electronic property of bound quinone. In addition, the adducts are rendered completely nonfluorescent as a result of an efficient, intracomplex electron transfer from photoexcited **1** to bound quinone. Thus, the abilities of quinones to quench fluorescence of porphyrin **1** are related not with their redox properties but with their abilities to bind to **1**; **6** ≅ **12** > **17** > **8** > **11** > **5**. The present host-guest complexation is discussed from the viewpoint of noncovalent strategy for the construction of biologically significant structures.

Quinone derivatives play an essential role as electron mediators in the charge separation processes in photosynthesis.[3] A variety of *covalently* linked porphyrin-quinone derivatives have been prepared and photoinduced electron transfer therein investigated as models of photosynthetic electron transfer.[4] This is along a typical line of biomimetic chemistry, a popular methodology of which is assembly of supposedly essential components via covalent linkage. In the present work, we have taken a different strategy to construct face-to-face porphyrin-quinone architectures. This is based on *noncovalent interaction*.[5] *cis*-Bis(2-hydroxynaphthyl)porphyrin **1** spontaneously forms such face-to-face adducts with *p*-quinones.[6] We report here on the details of this complexation, focusing upon (1) the structure-stability correlation from the viewpoint of molecular recognition of quinones and (2) the electronic interaction and photoinduced electron transfer in the adducts in relevance to the function of porphyrin-quinone architectures.

Chart I

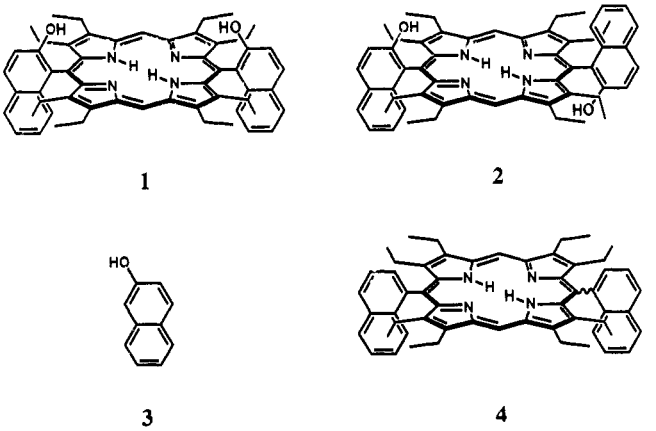

Results and Discussion

Two-Point Hydrogen-Bonding Fixation of *p*-Quinones. The interactions of various quinones with 5,15-*cis*-bis(2-hydroxy-1-naphthyl)octaethylporphyrin (**1**) as well as its trans isomer **2**, 2-naphthol (**3**), and dinaphthyl derivative **4** as references in

[†] Nagaoka University of Technology.
[‡] Kyoto University.

(1) Molecular Recognition. 16. Part 15: Kikuchi, Y.; Kato, Y.; Tanaka, Y.; Toi, H.; Aoyama, Y. *J. Am. Chem. Soc.* **1991**, *113*, 1349.

0002-7863/91/1513-6233$02.50/0

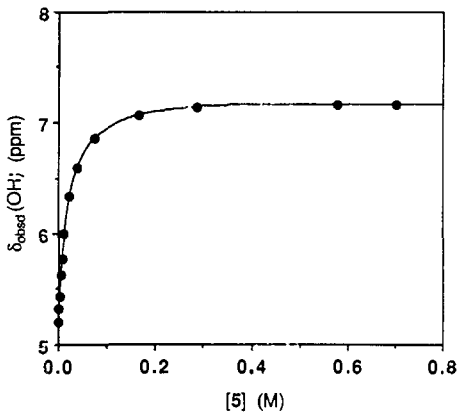

Figure 1. Correlation of chemical shifts of the OH groups of host **1** (δ_{obsd}(OH)) in $CDCl_3$ with [**5**]; $[\mathbf{1}]_t = 5.0 \times 10^{-3}$ M.

Chart II

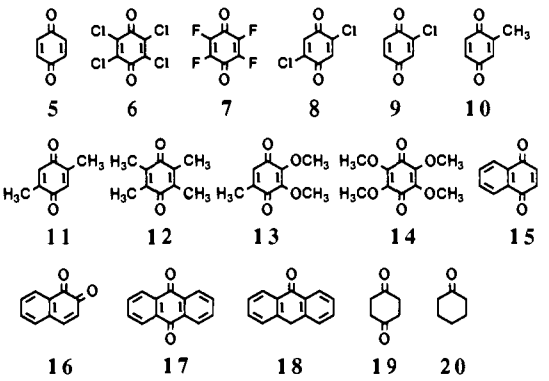

chloroform were investigated by means of ^{1}H NMR and IR spectroscopy (Chart I). The quinones employed were 1,4-benzoquinone (**5**) and its tetrachloro (chloranil, **6**), tetrafluoro (fluoranil, **7**), 2,5-dichloro (**8**), 2-chloro (**9**), 2-methyl (**10**), 2,5-dimethyl (**11**), tetramethyl (duroquinone, **12**), 2,3-dimethoxy-5-methyl (coenzyme Q_0, **13**), and tetramethoxy (**14**) derivatives, 1,4- (**15**) and 1,2-naphthoquinone (**16**), and 9,10-anthraquinone (**17**). The binding properties of anthrone (**18**) as monocarbonyl reference as well as 1,4-cyclohexanedione (**19**) and cyclohexanone (**20**) as aliphatic counterparts were also studied (Chart II).

The ^{1}H NMR spectrum of an approximately equimolar mixture of porphyrin **1** (5.0×10^{-3} M) and quinone **5** (5.1×10^{-3} M) in $CDCl_3$ at 298 K showed a sharp and single resonance for downfield-shifted OH protons of **1** (δ(OH) 5.62 with **5** and 5.20 without **5**) and an upfield-shifted proton resonance for **5** (δ(H) 5.92 with **1** and 6.72 without **1**). The change in δ(OH) for **1** with increasing molar ratios [**5**]/[**1**] exhibited a saturation behavior as shown in Figure 1. A $CHCl_3$ solution of **1** (5×10^{-3} M) showed ν(OH) at 3523 cm^{-1}. Upon addition of an equimolar amount of quinone **5**, a new absorption appeared at ν(OH) = 3448 cm^{-1}. The intensity ratios of the new to original absorption bands increased with increasing molar ratios [**5**]/[**1**].

These results indicate that porphyrin **1** and quinone 5 reversibly form a symmetrical face-to-face adduct **21** via a two-point hydrogen-bonding interaction between the hydroxyl groups of **1** and the carbonyl groups of **5**. The hydrogen bonding is evidenced by the significant shift (75 cm^{-1}) to lower wavenumber in ν(OH) and the large (~2 ppm, Figure 1) downfield shift of δ(OH), in a manner similar to that for related amino ester complexes.[7] On the other hand, an upfield shift of the ^{1}H NMR resonance for quinone **5** is undoubtedly due to ring-current effects of the porphyrin macrocycle,[8] and is thus consistent with structure **21**. The face-to-face geometry is consistent with the *single* resonances observed for both δ(OH) for **1** and δ(H) for **5**.[9]

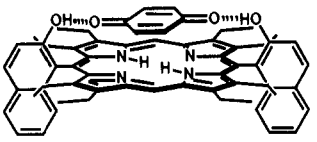

21

Other quinones **6**–**17** and references **18**–**20** also formed more or less stable complexes with host **1**, as evidenced by the characteristic downfield shifts of δ(OH) and shifts to lower wavenumbers in ν(OH). In cases of the binding of duroquinone (**12**) and 1,4-naphthoquinone (**15**) were also observed complexation-induced, large upfield shifts of the guest ^{1}H resonances. The spectral data are summarized in Table III (vide infra).

Binding Constants and Selectivities. The binding constants K were determined by ^{1}H NMR titration of host **1** ($\sim 5 \times 10^{-3}$ M) with guests in $CDCl_3$ (K = [complex]/[**1**][guest], eq 1). When free host and complex are in rapid equilibrium, their respective NMR signals for the OH groups are weighed-averaged to give the observed, sharp and single resonance; $\delta_{obsd}(OH) = \delta_1(OH)f_1$

$$\text{host} + \text{guest} \overset{K}{\rightleftharpoons} \text{complex} \qquad (1)$$

$+ \delta_{comp}(OH)(1 - f_1)$, where δ_1(OH) and δ_{comp}(OH), respectively, are the chemical shifts for free host **1** and **1**–guest complex and f_1 is the fraction of free host ($f_1 = [\mathbf{1}]/[\mathbf{1}]_t$; t = total). Under the Benesi–Hildebrand conditions ($[\text{guest}]_t/[\mathbf{1}]_t \geq 10$),[10] δ_{obsd}(OH) and $[\text{guest}]_t$ are correlated as shown in eq 2, where $\Delta\delta_{obsd}$(OH)

$$\frac{1}{\Delta\delta_{obsd}(OH)} = \frac{1}{\Delta\delta_{comp}(OH)} + \frac{1}{K}\frac{1}{\Delta\delta_{comp}(OH)}\frac{1}{[\text{guest}]_t} \qquad (2)$$

$= \delta_{obsd}(OH) - \delta_1(OH)$ and $\Delta\delta_{comp}(OH) = \delta_{comp}(OH) - \delta_1(OH)$. Plots of $1/\Delta\delta_{obsd}(OH)$ vs $1/[\text{guest}]_t$ give a straight line and the two unknowns, K and $\Delta\delta_{comp}(OH)$, are obtained from the slope and intercept. When the Benesi–Hildebrand conditions are not strictly satisfied, the binding constants can be evaluated either directly from the knowledge of saturation-binding data or by the Lang's modification of the Benesi–Hildebrand treatment.[11] The binding constants thus obtained at 298 K and other temperatures and the associated thermodynamic parameters are summarized in Tables I and II, respectively. In Table III are shown the values for $\Delta\delta_{comp}$(OH) and the shifts to lower wavenumbers in ν(OH) upon complex formation ($\Delta\nu_{comp}(OH) = \nu_1(OH) - \nu_{comp}(OH)$).

The complexation equilibria between selected guests and trans porphyrin **2** or 2-naphthol (**3**) as reference host were also followed

(2) Present address: Section of Bioorganic Chemistry, Department of BioEngineering, Nagaoka University of Technology.

(3) (a) Deisenhofer, J.; Epp, O.; Miki, K.; Huber, R.; Michel, H. *J. Mol. Biol.* **1984**, *180*, 385. (b) Deisenhofer, J.; Epp, O.; Miki, K.; Huber, R.; Michel, H. *Nature (London)* **1985**, *318*, 618. (c) Michel, H.; Epp, O.; Deisenhofer, J. *EMBO J.* **1986**, *5*, 2445.

(4) Review: Borovkov, V. V.; Evstigneeva, R. P.; Strekova, L. N.; Filippovich, E. I. *Russ. Chem. Rev. (Engl. Transl.)* **1989**, *58*, 1032.

(5) For a recent example of similar approaches, see: Tecilla, P.; Dixon, R. P.; Slobodkin, G.; Alavi, D. S.; Waldeck, D. H.; Hamilton, A. D. *J. Am. Chem. Soc.* **1990**, *112*, 9408.

(6) For the use of porphyrins as hosts in the hydrogen-bonded complex formation, see: (a) Hamilton, A. D.; Lehn, J.-M.; Sessler, J. L. *J. Am. Chem. Soc.* **1986**, *108*, 5158. (b) Lindsey, J. S.; Kearney, P. C.; Duff, R. J.; Tjivikua, P. T.; Rebek, J., Jr. *Ibid.* **1988**, *110*, 6575. (c) Aoyama, Y.; Asakawa, M.; Yamagishi, A.; Toi, H.; Ogoshi, H. *Ibid.* **1990**, *112*, 3145.

(7) Aoyama, Y.; Yamagishi, A.; Asakawa, M.; Toi, H.; Ogoshi, H. *J. Am. Chem. Soc.* **1988**, *110*, 4076.

(8) (a) Ogoshi, H.; Setsune, J.; Omura, T.; Yoshida, Z. *J. Am. Chem. Soc.* **1975**, *97*, 6461. (b) Abraham, R. J.; Fell, S. C. M.; Smith, K. M. *Org. Magn. Reson.* **1977**, *9*, 367.

(9) The observation of a single benzoquinone resonance may simply reflect the fast exchange between two edge-to-face conformations. This is, however, unlikely, although not rigorously ruled out, for the following reasons. First, an examination of CPK molecular models for adduct **1·5** (**21**) indicates that the two rings are too close to allow an edge-to-face conformation. Second, as is described in the later part of the text, the electronic spectrum of the benzoquinone adduct is essentially the same as that of the anthraquinone adduct, which can take only a face-to-face conformation.

(10) Benesi, H.; Hildebrand, J. H. *J. Am. Chem. Soc.* **1949**, *71*, 2703.

(11) Lang, R. P. *J. Am. Chem. Soc.* **1962**, *84*, 1185.

Table I. Binding Constants (K, M^{-1}) for the Host–Guest Complexation in $CDCl_3$[a]

host	guest	T (K) 243	258	273	298[b]	313	328
1	5	4.8×10^2	2.4×10^2	1.3×10^2	5.5×10		
	6				4.0×10^2	1.8×10^2	1.0×10^2
	7				3.7×10^2	2.0×10^2	1.1×10^2
	8	5.6×10^3	1.5×10^3	6.5×10^2	2.2×10^2		
	9	1.4×10^3	5.7×10^2	3.1×10^2	1.2×10^2		
	10	9.6×10^2	4.5×10^2	2.4×10^2	8.8×10		
	11	1.4×10^3	6.0×10^2	3.3×10^2	1.1×10^2		
	12				4.2×10^2	1.7×10^2	9.0×10
	13				3.5×10	2.1×10	1.3×10
	14	4.0×10	2.7×10	1.7×10	7.8		
	15	3.9×10^3	5.1×10^2		1.7×10^2		
	16		1.7×10	1.3×10	8.7		
	17	9.0×10^3	2.0×10^3	8.6×10^2	2.3×10^2		
	18		1.6×10	1.2×10	4.2		
	19		2.2×10	1.7×10	1.0×10		
	20		3.8×10^{-1}	3.2×10^{-1}	2.4×10^{-1}		
2	5	1.3×10	8.2	5.4	3.2		
	12	1.4×10	8.8	5.8	3.0		
	17	3.1×10	2.1×10	1.3×10	5.9		
	18	2.3×10	1.2×10	7.9	4.5		
3	5	4.2	3.1	2.4	1.9		
	12				2.3		
	17	1.5×10	9.6	7.6	3.9		

[a] Errors in K's are ≤10%. [b] The K's determined by UV/visible titration at 298 K for $CHCl_3$ solutions are 4.5×10 (**5**), 8.0 (**14**), 2.0×10^2 (**17**), and 4.7 M^{-1} (**18**).

Table II. Thermodynamic Parameters for the Host–Guest Complexation in $CDCl_3$[a]

host	guest	$\Delta G°_{298}$ (kcal/mol)	$\Delta H°$ (kcal/mol)	$T\Delta S°_{298}$ (kcal/mol)
1	5	−2.4	−5.6	−3.3
	6	−3.6	−8.6	−5.1
	7	−3.5	−8.0	−4.5
	8	−3.1	−8.4	−5.3
	9	−2.8	−6.5	−3.7
	10	−2.7	−6.3	−3.6
	11	−2.8	−6.8	−4.0
	12	−3.6	−9.0	−5.5
	13	−2.1	−6.0	−4.0
	14	−1.2	−4.3	−3.1
	15	−3.0	−8.3	−5.3
	16	−1.3	−2.6	−1.3
	17	−3.2	−7.9	−4.7
	18	−0.89	−5.2	−4.3
	19	−1.4	−2.9	−1.5
	20	0.86	−1.8	−2.6
2	5	−0.69	−3.6	−2.9
	12	−0.65	−4.1	−3.4
	17	−1.1	−3.8	−2.6
	18	−0.90	−4.1	−3.2
3	5	−0.39	−2.7	−2.4
	12	−0.49		
	17	−0.85	−3.4	−2.5

[a] Free energy ($\Delta G°$) and entropy changes ($T\Delta S°$) are at 298 K.

by similar ^1H NMR titration at 298 K and other temperatures. The binding constants and thermodynamic parameters are also shown in Tables I and II, respectively.

(a) Selectivities between Two-Point and One-Point Hydrogen-Bonding Interactions. The strength of a hydrogen bond can be evaluated by $\Delta\delta_{comp}(OH)$ and $\Delta\nu_{comp}(OH)$ values. Anthraquinone (**17**) and anthrone (**18**) form very similar hydrogen bonds with host **1**, as judged on this criterion (Table III). A clear indication for the importance of two-point interaction comes from comparison of the binding constants at 298 K of **17** and **18** (Table I). The two-point host **1** binds **17** 54 times more strongly than **18** (K_1(**17**)/K_1(**18**) = 54), while one-point reference host **2** shows almost no discrimination between **17** and **18** (K_2(**17**)/K_2(**18**) = 1.3). Although, in a different viewpoint, **18** shows a slight preference for **2** over **1** (K_1(**18**)/K_2(**18**) = 0.93), **17** is bound more tightly with **1** than with **2** by a factor of 38 (K_1(**17**)/K_2(**17**) = 38). These results indicate that the *second* hydrogen bond in the two-point

Table III. Spectral Data for the Adducts of Host **1** and Guests and One-Electron Reduction Potentials ($E°$) of Guest Quinones

guest	$\Delta\delta_{comp}(OH)$[a] (ppm)	$\Delta\nu_{comp}(OH)$[b] (cm^{-1})	λ_{max}[c,d] (nm)	$E°$[e] (V vs SCE)
5	2.00	75	626	−0.51
6	1.80	36	623	0.01
7	1.38	30	623	−0.04
8	1.79	56		−0.18
9	1.91	66		−0.34
10	2.14	81		−0.58
11	2.26	87		−0.67
12	2.61	97	632	−0.84
13	2.03	89		−0.71
14	2.00	89	628	−0.69[f]
15	2.44	94		−0.71
16	2.20			
17	2.85	102	628	−0.94
18	2.72	101	629	
19	1.87			
20	2.50			

[a] Downfield shifts for δ(OH) of **1** upon complexation in $CDCl_3$; $\Delta\delta_{comp}(OH) = \delta_{comp}(OH) - \delta_1(OH)$. [b] Shifts to lower wavenumbers in ν(OH) of **1** upon complexation in $CHCl_3$; $\Delta\nu_{comp}(OH) = \nu_1(OH) - \nu_{comp}(OH)$. [c] For the longest wavelength absorption band of **1** in $CHCl_3$ in the presence of a large excess amount of guest quinone to assure >70% complexation. [d] In the absence of any guest, **1** shows λ_{max} at 627 nm. [e] For CH_3CN solutions (ref 15). [f] This work.

Scheme I

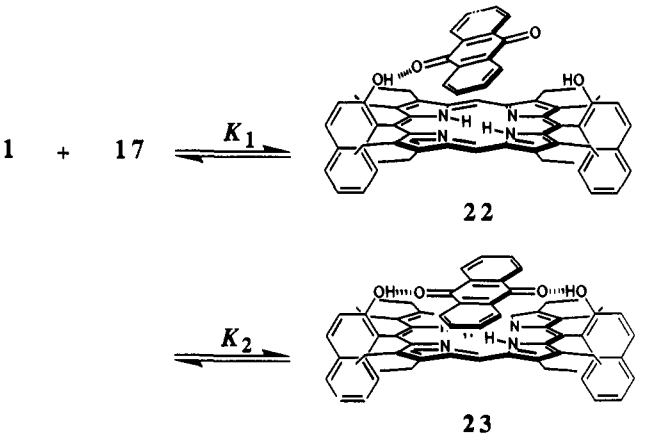

22 **23**

Chart III

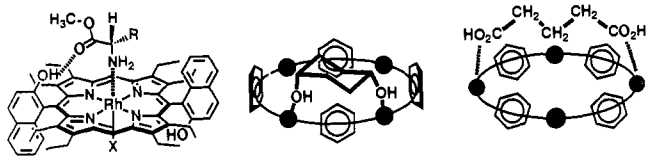

24 25 26

adduct **1·17** (**23**; Scheme I) gives rise to a selectivity of K_2 = 54/1.3 = 38/0.93 = 41.[12]

The selectivity factor K_2 actually is the equilibrium constant for the intramolecular hydrogen bonding in one-point adduct **22** (K_2 = [**23**]/[**22**], Scheme I). This hydrogen bond shows a remarkable similarity, from both thermodynamic and spectroscopic viewpoints, to the related, intramolecular hydrogen bond between hydroxyl and ester groups in the two-point amino ester adduct **24** (Chart III): For **23**, K_2 = 41 ($-\Delta G°_2 = RT \ln 41$ = 2.2 kcal/mol) at 298 K, $\Delta\delta_{comp}$(OH) = 2.85 ppm, and $\Delta\nu_{comp}$(OH) = 102 cm^{-1}; for **24**, K_2 = 42 ($-\Delta G°_2 = RT \ln 42$ = 2.1 kcal/mol) at 288 K, $\Delta\delta_{comp}$(OH) = ~3 ppm, and $\Delta\nu_{comp}$(OH) = ~100 cm^{-1}.[7] The equilibrium constant for the first, *intermolecular* hydrogen bonding (K_1 = [**22**]/[**1**][**17**]; Scheme I) is evaluated from the relationship $K_1 = K_1(\mathbf{17})/K_2$ = 5.5 M^{-1}.

The quantity $K_1(\mathbf{17})/(K_1)^2$ = 7.4 M^{-1} corresponds to the extent to which the intramolecular K_2 process is *entropically* more favorable than the intermolecular K_1 process; $RT \ln [K_1(\mathbf{17})/(K_1)^2] = -(\Delta G°1 + \Delta G°_2) + 2\Delta G°_1 = \Delta G°_1 - \Delta G°_2 = (T\Delta S_2 - T\Delta S_1)$ = 1.2 kcal/mol (298 K), if it is assumed that the enthalpy changes for the K_1 and K_2 processes are the same.[12] The calculated value (1.2 kcal/mol) is in agreement with those for two-point hydrogen-bonded diol complex **25** (1.3 kcal/mol)[13] and dicarboxylic acid complex **26** (1.9 kcal/mol)[14] of resorcinol–dodecanal cyclotetramer, which has four pairs of hydrogen-bonded OH groups (schematically shown by filled circles in structures **25** and **26**) as the sites of guest binding. This generalization is remarkable, since there is a very large span in the overall binding constants themselves; 2.3 × 10^2 for **23**, 1.04 × 10^3 for **25**, and 1.2 × 10^5 M^{-1} for **26**.

1,2-Naphthoquinone (**16**) cannot form simultaneous two-point hydrogen bonds with **1**. This is responsible for the observed difference in the affinities of **16** and its 1,4-isomer **15**; $K_1(\mathbf{15})/K_1(\mathbf{16})$ = 19 at 298 K. There is also a remarkable discrimination between aliphatic 1,4-diketone **19** and monoketone **20**; $K_1(\mathbf{19})/K_1(\mathbf{20})$ = 44.

(b) Factors Affecting the Stabilities of Adducts. In Table III are included the one-electron reduction potentials ($E°$) for *p*-quinones,[15] in acetonitrile solutions, as measures of their basicities. In Figure 2 are plotted $\Delta\nu_{comp}$(OH) and $\Delta\delta_{comp}$(OH) for *p*-quinones against $E°$. The satisfactory correlations observed indicate that the less readily reducible, and hence more basic, quinones form the stronger hydrogen bonds with host **1**.

The binding constants decrease on going from anthra- (**17**) through naphtho- (**15**) to benzoquinone (**5**) (Table I). This order apparently points to the importance of porphyrin–quinone π–π stacking interaction[16] but does not necessarily do so. It may simply reflect the strengths of hydrogen bonds involved ($\Delta\nu_{comp}$(OH) and $\Delta\delta_{comp}$(OH)) in the decreasing order **17** > **15** > **5**. The binding constants of quinones **5** and **17** for one-point reference hosts **2** and **3** (Table I) provide other good comparisons. The preference for porphyrin host **2** over non-porphyrin host **3** may reflect stacking interaction and is only moderate; $K_2(\mathbf{5})/K_3(\mathbf{5})$ = 1.7 or $K_2(\mathbf{17})/K_3(\mathbf{17})$ = 1.5 at 298 K. Furthermore, the selectivity of **2** for **17** over **5** is almost the same as that of **3**; $K_2(\mathbf{17})/K_2(\mathbf{5})$ = 1.8 and $K_3(\mathbf{17})/K_3(\mathbf{5})$ = 2.0. These results indicate that porphyrin–quinone π–π stacking interaction, if any, makes only a minor contribution to the *stabilities* of adducts. This is in accord with a literature report that the porphyrin–quinone π–π interaction is weak.[17] In fact, singly linked porphyrin–quinone derivatives adopt open or unfolded conformations.[18]

The binding constants for substituted benzoquinones **6**–**14** exhibit a complicated pattern. Methyl-substituted derivatives **10**–**12** are more basic than benzoquinone (**5**) (cf. $E°$ values). As a consequence, they form stronger hydrogen bonds with host **1** than **5** (referring to $\Delta\nu_{comp}$(OH) and $\Delta\delta_{comp}$(OH)), and the stabilities of the resulting adducts decrease in the order **1·12** > **1·11** > **1·10** > **1·5** (Table I). Chloranil (**6**) and fluoranil (**7**), on the

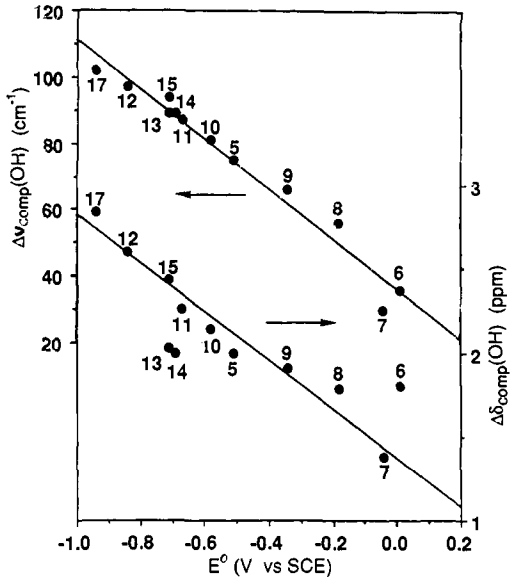

Figure 2. Correlation of complexation-induced downfield shifts of the OH proton resonances ($\Delta\delta_{comp}$(OH)) and shifts to lower wavenumbers in the O–H stretching vibration frequencies ($\Delta\nu_{comp}$(OH)) of host **1** with one-electron reduction potentials ($E°$) of guest quinones in $CHCl_3$.

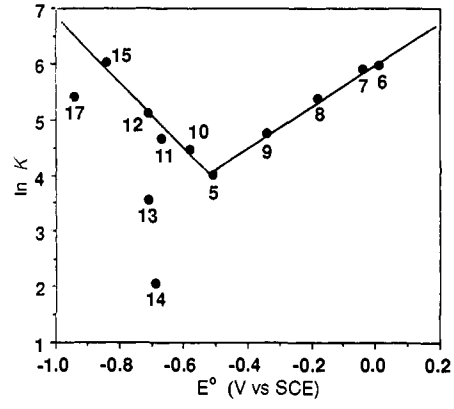

Figure 3. Correlation of logarithmic binding constants (ln K) with one-electron reduction potentials ($E°$) of guest quinones for the complexation of host **1** and *p*-quinones in $CDCl_3$ at 298 K.

(12) These analyses of the binding data are not so strict as in the previous cases of the binding of bifunctonal guests. The reason for this is that the two carbonyl groups of a quinone are not *independent* from each other but are conjugated, in marked contrast to aliphatic diols[13] and dicarboxylic acids[14] having two binding sites that are separated by aliphatic chains.

(13) Reference in note 1.

(14) Tanaka, Y.; Kato, Y.; Aoyama, Y. *J. Am. Chem. Soc.* **1990**, *112*, 2809.

(15) (a) Fukuzumi, S.; Koumitsu, S.; Hironaka, K.; Tanaka, T. *J. Am. Chem. Soc.* **1987**, *109*, 305. (b) Fukuzumi, S.; Ishikawa, M.; Tanaka, T. *J. Chem. Soc., Perkin Trans. 2* **1989**, 1811. (c) Morrison, L. E.; Schelhorn, J. E.; Cotton, T. M.; Bering, C., L.; Loach, P. A. In *Function of Quinones in Energy Conserving Systems*; Trumpower, B. L., Ed.; Academic Press: New York, 1982; pp 35–58.

(16) (a) Williams, K.; Askew, B.; Ballester, P.; Buhr, C.; Jeong, K. S.; Jones, S.; Rebek, J., Jr. *J. Am. Chem. Soc.* **1989**, *111*, 1090. (b) Hamilton, A. D.; Van Engen, D. *Ibid.* **1987**, *109*, 5035. (c) Zimmerman, S. C.; Wu, W. *Ibid.* **1989**, *111*, 8054.

(17) Hunter, C. A.; Sanders, K. M. *J. Am. Chem. Soc.* **1990**, *112*, 5525.

(18) Gust, D.; Moore, T. A.; Liddell, P. A.; Nemeth, G. A.; Makings, L. R.; Moore, A. L.; Barrett, D.; Pessik, P. J.; Benasson, R. V.; Rougee, M.; Chachaty, C.; De Schryver, F. C.; Van der Auweraer, M.; Holzwath, A. R.; Connolly, J. S. *J. Am. Chem. Soc.* **1987**, *109*, 846.

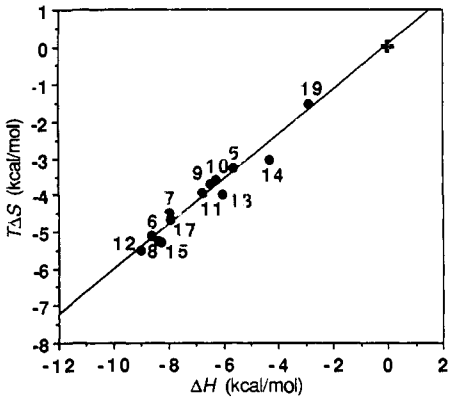

Figure 4. Correlation of enthalpy changes ($\Delta H°$) with entropy changes ($T\Delta S°$) at 298 K for the complexation of host **1** and *p*-quinones in $CDCl_3$. The cross mark indicates the origin.

other hand, are less basic than **5** and in fact form weaker hydrogen bonds than **5**. Nevertheless, adducts **1·6** and **1·7** are significantly more stable than **1·5**; $K_1(\mathbf{6})/K_1(\mathbf{5}) = 7.3$ and $K_1(\mathbf{7})/K_1(\mathbf{5}) = 6.7$. Dichloro (**8**) and monochloro (**9**) derivatives exhibit intermediate behaviors ($E°$, $\Delta\delta_{comp}$(OH) and $\Delta\nu_{comp}$(OH), and K_1) between **6** and **5**. The stabilization of the adducts of halogen-substituted benzoquinones may be due to an electrostatic or the so-called charge-transfer interaction between the electron-deficient quinone nucleus and the electron-rich porphyrin macrocycle. Details, however, still remain to be further investigated.[19] The occurrence of two types of stabilization of both electron-rich and -deficient quinones is clearly shown by the V-shaped correlation of ln K with $E°$ for *p*-quinones (Figure 3), where the minimum occurs at quinone **5**.

Examination of CPK molecular models for the face-to-face adduct of anthraquinone **1·17** (**23**; Scheme I) indicates a steric contact between the benzo moiety of bound **17** and the peripheral ethyl groups of porphyrin **1**. Methoxy-substituted benzoquinones **13** and **14** are subject to a more pronounced steric interaction between *bent* OCH_3 groups and the porphyrin plane. These are probably why quinones **17**, **13**, and **14** exhibit deviations in the ln K vs $E°$ correlation (Figure 3). Steric depression of complexation seems to be also important in the case of cyclohexane derivatives **19** and **20**, which have axial hydrogens. The complexation of quinones with reference host **3** is free from any large steric effects. In this case, the binding constants decrease simply in the order $K_3(\mathbf{17}) > K_3(\mathbf{12}) > K_3(\mathbf{5})$ (Table I), i.e., the order of decreasing basicities of quinones ($E°$, Table III).

Tight binding usually results in loss of motional freedom. In fact, approximately 60% of the gain in enthalpy change ($\Delta H°$) is canceled by entropy loss ($T\Delta S°$) (Table II). There is also a compensation between $\Delta H°$ and $T\Delta S°$ (T = 298 K) for the complexation of host **1** with *p*-quinones, as shown in Figure 4. This correlation also includes the data for the two-point reference guest **19**. The best fit, least-squares line is $T\Delta S° = 0.60\Delta H°$ (r = 0.97), so that $\Delta G° = 0.40\Delta H°$ (298 K). Such an enthalpy–entropy compensation is often observed for the cation binding with crown ethers and related macrocycles.[20] The present results indicate that this is also true for the host–guest complexation based on multiple interaction involving the hydrogen bonding.

Face-to-Face Separation and Electronic Interaction. CPK molecular models for adduct **1·5** (**21**) indicate that the benzene and quinone rings are almost in contact, having a face-to-face separation of approximately 3 Å. The ^{1}H NMR signal for quinone **5** underwent an upfield shift in the presence of porphyrin **1** (vide supra). Titration of **5** with varying amounts of **1**, followed by Benesi–Hildebrand analysis of the chemical shifts, allowed determination of the complexation-induced upfield shift of protons

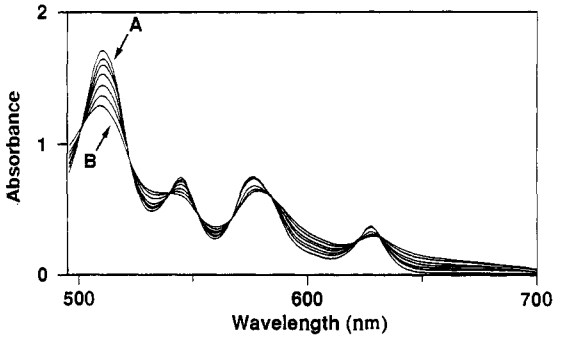

Figure 5. Electronic absorption spectra in the region of 500–700 nm of host **1** (1.0×10^{-4} M) in $CHCl_3$ in the presence of varying amounts of quinone **17**; [**17**] = 0, 5.0×10^{-4}, 1.0×10^{-3}, 2.0×10^{-3}, 5.0×10^{-3}, 1.0×10^{-2}, and 2.0×10^{-2} M, read from A to B.

Chart IV

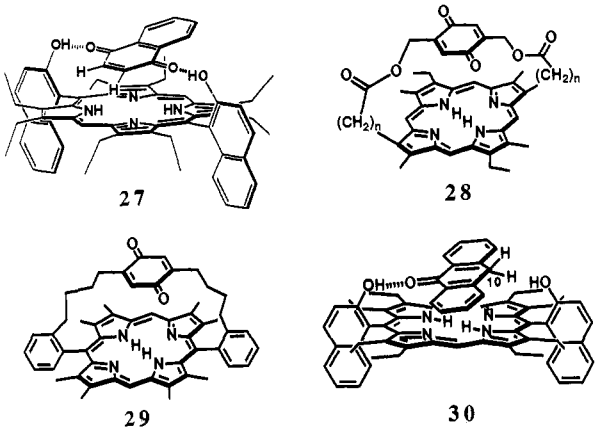

of bound **5** ($\Delta\delta_{comp}$(H) = 4.86 ppm) and the binding constant (K = 4.9×10 M^{-1} at 298 K). The latter is in excellent agreement with the binding constant, $K_1(\mathbf{5}) = 5.5 \times 10$ M^{-1} at 298 K (Table I), obtained by titration of host **1** with guest **5**. Similar titration of naphthoquinone (**15**) and duroquinone (**12**) gave $\Delta\delta_{comp}$(H) = 5.08 ppm for the 2-H and 3-H of bound **15** and $\Delta\delta_{comp}(CH_3)$ = 2.22 ppm for the methyl protons of bound **12**. A more pronounced upfield shift for **15** over **5** suggests a tilting of bound **15** around the hydrogen-bond axis (structure **27**; Chart IV) so that 2-H and 3-H are closer to the porphyrin plane. This may be due to steric interaction between the benzo group of **15** and the ethyl groups of the porphyrin, as also suggested above for the anthraquinone adduct **1·17** (**23**; Scheme I). CPK models indicate that the benzo group lies above the porphyrin periphery. In support of this, the meso protons of adduct **23** showed a complexation-induced upfield shift of 0.7 ppm as a result of ring-current effects of the benzo groups of bound **17**.

There are a number of literature reports on covalently double linked face-to-face porphyrin–quinone derivatives.[21] Two examples are shown below. Compound **28** (n = 2), the shortest bridge member of the family, exhibits an upfield shift of 4 ppm for the quinone nucleus protons.[22] CPK molecular models for **28** suggest a face-to-face separation of 4–4.5 Å. Compound **29** has the shortest face-to-face distance of 3.42 Å (X-ray crystallography).[23] The present two-point adducts **1·5** and **1·15** with $\Delta\delta_{comp}$(H) ≅ 5 ppm for the quinone nucleus protons probably have

(19) For a recent discussion on the nature of π–π interactions, see ref 17.

(20) (a) Izatt, R. M.; Terry, R. E.; Haymore, B. L.; Hansen, L. D.; Daley, N. K.; Avondet, A. G.; Christensen, J. J. *J. Am. Chem. Soc.* **1976**, *98*, 7620. (b) Michaux, G.; Reisse, J. *Ibid.* **1982**, *104*, 6895. (c) Ouchi, M.; Inoue, Y.; Kanzaki, T.; Hakushi, T. *J. Org. Chem.* **1984**, *49*, 1408.

(21) (a) Lindsey, J. S.; Mauzerall, D. C. *J. Am. Chem. Soc.* **1982**, *104*, 4498. (b) Lindsey, J. S.; Mauzerall, D. C. *Ibid.* **1983**, *105*, 6528. Lindsey, J. S.; Delaney, J. K.; Mauzerall, D. C.; Linschitz, H. *Ibid.* **1988**, *110*, 3610. (d) Osuka, A.; Furuta, H.; Maruyama, K. *Chem. Lett.* **1986**, 479. (e) Weiser, J.; Staab, H. A. *Angew. Chem., Int. Ed. Engl.* **1984**, *23*, 623.

(22) (a) Ganesh, K. N.; Sanders, J. K. M. *J. Chem. Soc., Chem. Commun.* **1980**, 1129. (b) Ganesh, K. N.; Sanders, J. K. M. *J. Chem. Soc., Perkin Trans. 1* **1982**, 1611. (c) Ganesh, K. N.; Sanders, J. K. M.; Waterton, J. C. *J. Chem. Soc., Perkin Trans. 1* **1982**, 1617.

(23) (a) Krieger, C.; Weiser, J.; Staab, H. A. *Tetrahedron Lett.* **1985**, *26*, 6055. (b) Weiser, J.; Staab, H. A. *Ibid.* **1985**, *26*, 6059.

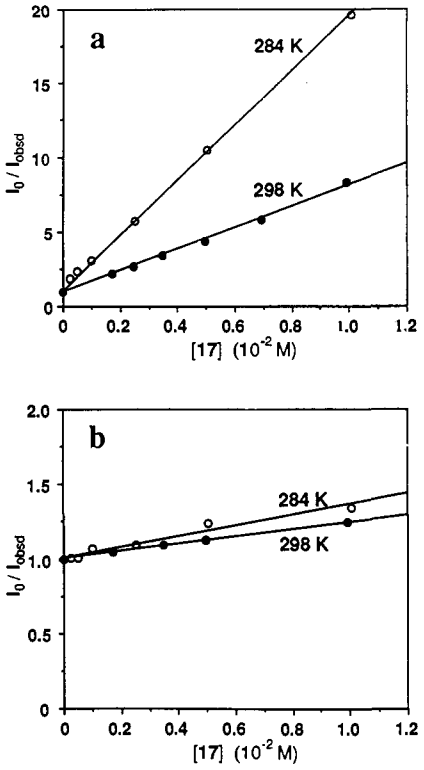

Figure 6. Stern–Volmer plots for the fluorescence quenching of hosts **1** (a) and **4** (b) with quinone **17** in benzene at 298 and 284 K: exitation at 544 nm, emission at 633 nm for **1** or 634 nm for **4**, and [**1**] = [**4**] = 1.0×10^{-5} M.

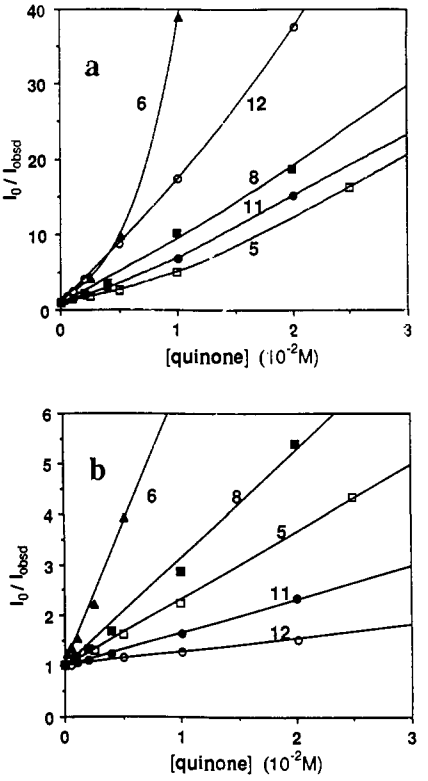

Figure 7. Stern–Volmer plots for the fluorescence quenching of hosts **1** (a) and **4** (b) with quinones **5**, **6**, **8**, **11**, and **12** in benzene at 298 K: exitation at 544 nm, emission at 633 nm for **1** or 634 nm for **4**, and [**1**] = [**4**] = $\sim 1.0 \times 10^{-5}$ M.

the shortest (~3 Å, judging from CPK models) face-to-face distance ever known, although evaluation of face-to-face distances from the NMR shifts requires information about edge-on contributions to the face-to-face conformations. Such a close proximity of the porphyrin and quinone rings in fact results in their significant electronic interaction.

Figure 5 shows the electronic absorption spectra, in the region of 500–700 nm, of host **1** in the presence of varying amounts of anthraquinone (**17**) in $CHCl_3$. The observation of clear isosbestic points confirms a 1:1 complexation (eq 1). The binding constant was evaluated by the Benesi–Hildebrand analysis of the absorbance change at, e.g., 510 nm; $K = 2.0 \times 10^2$ M^{-1} at 298 K, in agreement with K_1(**17**) = 2.3×10^2 M^{-1} at 298 K obtained by NMR titration. Titration of **1** with **17** in benzene gave $K = 5.1 \times 10^2$ M^{-1}. For benzoquinone (**5**), $K = 4.5 \times 10$ M^{-1} (in $CHCl_3$) and 1.4×10^2 M^{-1} (in benzene). The solvent dependence of K is reasonable in view of promotion of hydrogen bonding in less polar solvents. The binding constants for other selected guests were obtained by similar UV/visible titration and are shown in a footnote of Table I.

Upon adduct formation, all of the absorption bands of **1** undergo significant broadening. Especially, the tailing of the longest wavelength band extends into >700 nm. The absorption maximum (λ_{max}) of this band depends on the nature of bound quinone, and decreases in the order **12** > **14** ≅ **17** ≅ **18** > **5** > **6** ≅ **7** (Table III). This order is roughly parallel to the decreasing order of quinone basicities as reflected on $E°$ values (Table III), indicating that the interaction between the porphyrin and quinone π systems in an enforced proximity is at least partially of the charge-transfer type.

Electronic absorption spectroscopy applied to reference systems can be used to solve some fundamental questions. The first is cyclohexanedione (**19**), an aliphatic reference. This guest in a great excess amount (0.16 M) to assure approximately 60% complexation of host **1** led to practically no change in the electronic spectrum of **1**. A π system in bound guest is thus essential for the perturbation of the π electronic structure of **1**. The second is anthrone (**18**), a one-point reference. Adduct **1·18** showed essentially the same spectrum as anthraquinone adduct **1·17** (Figure 5). This result strongly suggests that **1·18** takes a face-to-face conformation (structure **30**) as a result of *intramolecular* π–π stacking. This was also supported by ^{1}H NMR titration of **18** with porphyrin **1**, where the 10-H's of **18** underwent an upfield shift. Benesi–Hildebrand treatment of the data indicated a complexation-induced shift ($\Delta\delta_{comp}$(H)) of 3.69 ppm as a result of the ring-current effects of the porphyrin plane in adduct **1·18** (**30**). The third is dinaphthyl reference-host **4**, which has no hydrogen-bonding site. The electronic spectrum of this host remained practically unchanged in the presence of a large excess amount (0.1 M) of benzoquinone (**5**), chloranil (**6**), or anthraquinone (**17**). In addition, the ^{1}H NMR resonance of benzoquinone (**5**) underwent no upfield shift in the presence of host **4** (up to solubility limit). These results can be taken as evidence that the host–guest hydrogen-bonding is essential for the present complexation.

Photoinduced Electron Transfer. Quinones are known to quench porphyrin fluorescence by the mechanism involving electron transfer from photoexcited porphyrin to quinone.[24] Much effort has been devoted to the elucidation of geometrical requirements for efficient electron transfer.[25] To this end, a variety of covalently

(24) (a) Tabushi, I.; Koga, N.; Yanagita, M. *Tetrahedron Lett.* **1979**, *20*, 257. (b) Bergkamp, M. A.; Dalton, J.; Netzel, T. L. *J. Am. Chem. Soc.* **1982**, *104*, 253. (c) Schmidt, J. A.; McIntosh, A. R.; Weedon, A. C.; Bolton, J. R.; Connolly, J. S.; Hurley, J. K.; Wasielewski, M. R. *Ibid.* **1988**, *110*, 1733 and references therein. (d) Sessler, J. L.; Johnson, M. R.; Lin, T.-Y.; Creager, S. E. *Ibid.* **1988**, *110*, 3659. (e) Gust, D.; Moore, T. A.; Moore, A. L.; Makings, L. R.; Seely, G. R.; Ma, X.; Trier, T. T.; Gao, F. *Ibid.* **1988**, *110*, 7567. (f) Wasielewski, M. R.; Gaines, G. L., III; O'Neal, M. P.; Svec, W. A.; Niemczyk, M. P. *Ibid.* **1990**, *112*, 4559. (g) Sessler, J. L.; Capuano, V. L. *Angew. Chem., Int. Ed. Engl.* **1990**, *29*, 1134.

(25) (a) Joran, A. D.; Leland, B. A.; Geller, G. G.; Hopfield, J. J.; Dervan, P. B. *J. Am. Chem. Soc.* **1984**, *106*, 6090. (b) Wasielewski, M. R.; Niemczyk, M. P. *Ibid.* **1984**, *106*, 5043. (c) Wasielewski, M. R.; Niemczyk, M. P.; Svec, W. A.; Pewitt, E. B. *Ibid.* **1985**, *107*, 1080. (d) Leland, B. A.; Joran, A. D.; Felker, P. M.; Hopfield, J. J.; Zewail, A. H.; Dervan, P. B. *J. Phys. Chem.* **1985**, *89*, 5571. (e) Sakata, Y.; Nakashima, S.; Goto, Y.; Tatemitsu, H.; Misumu, S.; Asahi, T.; Hagihara, M.; Nishikawa, S.; Okada, T.; Mataga, N. *J. Am. Chem. Soc.* **1989**, *111*, 8979. (f) von Gersdorff, J.; Huber, M.; Schuberl, H.; Niethammer, D.; Kirste, B.; Plato, M.; Möbius, K.; Hurreck, H.; Eichberger, R.; Kiezmann, R.; Willig, F. *Angew. Chem., Int. Ed. Engl.* **1990**, *29*, 670.

linked porphyrin–quinone derivatives have been prepared.[4] The fluorescence quenching of the present porphyrin **1** as well as reference **4** by selected quinones **5**, **6**, **8**, **11**, **12**, and **17** was investigated for benzene solutions. The correlations between concentrations of anthraquinone (**17**) and extents of fluorescence quenching as expressed by I_0/I_{obsd} at 298 or 284 K are shown in Figure 6a (for **1**) and 6b (for **4**), where I_0 and I_{obsd} are the fluorescence intensities (in arbitrary unit) at 633 nm (for **1**) or 634 nm (for **4**) of the porphyrin excited at 544 nm in the absence and presence of quinone **17**, respectively. Similar correlations at 298 K with other quinones for porphyrins **1** and **4** are shown in Figure 7a and 7b, respectively.

The fluorescence quenching of reference **4** must be based on intermolecular collision of photoexcited **4** and a quinone molecule. Such being the case, I_0/I_{obsd} is correlated with [quinone] by the Stern–Volmer expression (eq 3),[26] where k_2 is the second-order

$$I_0/I_{obsd} = 1 + k_2\tau[\text{quinone}] \qquad (3)$$

rate constant for the quenching of excited **4** by the quinone and τ is the fluorescence lifetime of **4** in the absence of quencher. Thus, the slopes ($k_2\tau$) of I_0/I_{obsd} vs [quinone] plots (Figures 6b and 7b) represent relative k_2, and decrease in the order **6** (5.6×10^2) > **8** (2.1×10^2) > **5** (1.3×10^2) > **11** (0.66×10^2) > **12** (0.26×10^2) ≅ **17** (0.26×10^2 M^{-1}), i.e., the order of decreasing quinone basicities.

The quenching of porphyrin **1**, on the other hand, is significantly more efficient (Figures 6a and 7a) than that of reference **4** (Figures 6b and 7b), and is almost complete at higher concentrations of high-affinity quinones **6**, **8**, **12**, and **17** and at the lower temperature (Figure 6a); I_0/I_{obsd} of 20, for example, corresponds to 95% quenching. The I_0/I_{obsd} vs [quinone] plots (Figures 6a and 7a) exhibit curvature at higher quinone concentrations but are approximately linear at lower quinone concentrations (≤0.5×10^{-2} M); the slopes of such linear correlations decrease in the order **6** (16×10^2) ≅ **12** (15×10^2) > **17** (6.7×10^2) > **8** (6.0×10^2) > **11** (4.6×10^2) > **5** (3.1×10^2 M^{-1}). This order parallels the order of decreasing binding constants (K_1; Table I). These results clearly indicate that the **1**–quinone adducts are rendered nonfluorescent owing to an efficient, intracomplex electron transfer from photoexcited **1** to bound quinone in close vicinity.

The ratios of the above-described slopes of the I_0/I_{obsd} vs [quinone] plots for porphyrin **1** to those for reference **4** (Figures 6b and 7b) using the same quinones are 58 (**12**), 26 (**17** at 298 K), 7.0 (**11**), 3.0 (**6**), 2.8 (**8**), and 2.3 (**5**). These ratios represent the significances of prior porphyrin–quinone complexation for the efficient, photoinduced porphyrin-to-quinone electron transfer. Thus, the photoreduction of strongly oxidizing chloroquinones **6** and **8** takes place even without complexation with porphyrin. However, efficient photoreduction of weakly oxidizing duroquinone (**12**) and anthraquinone (**17**) requires prior adduct formation.

The I_0/I_{obsd} vs [quinone] correlation for porphyrin **1** is only for the purpose of comparison. The fluorescence data must be analyzed by the Benesi–Hildebrand treatment according to the equilibrium (eq 1) involving fluorescent free-porphyrin **1** and nonfluorescent adduct **1**–quinone. The contribution of intermolecular quenching of excited **1** by quinone complicates the system, and allows no simple analysis. For duroquinone (**12**) and anthraquinone (**17**), however, the intermolecular quenching may be negligible as compared with the intracomplex quenching so that the Benesi–Hildebrand treatment can be justified. Analysis of the data for **12** and **17** at 298 K along this line gave binding constants of $K = 1.5 \times 10^3$ M^{-1} for **12** and 6.5×10^2 M for **17**.[27] The latter is in agreement with $K = 5.1 \times 10^2$ M^{-1} obtained by UV/visible titration of **1** with **17** in benzene (vide supra).

Noncovalent Strategy for the Porphyrin–Quinone Architectures. The covalent route to a face-to-face porphyrin–quinone derivative requires a highly substituted quinone precursor **31** (Y = H or functional group), where substituents X provide the sites for covalent linkage to a suitably difunctionalized porphyrin. There

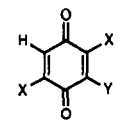

31

are two major difficulties in this covalent approach. The first is synthetic problems associated with the preparation of this type of tetra- or pentasubstituted benzene derivatives **31**. The preparation is multistep, and the yield of double coupling reaction is usually low. Second, there is little room for the systematic modification of the electronic/steric structures of quinones, since the side arms X are essential. On the other hand, the present, noncovalent strategy for the face-to-face porphyrin–quinone architectures takes advantage of a two-point hydrogen-bonding *interaction*, which is free from any difficulty associated with the double-coupling *reaction*. A 100% complexation with respect to porphyrin **1** can usually be achieved by use of a large excess amount of quinone or a low temperature. Most importantly, the four open positions of parent benzoquinone (**5**) can be freely used for the preparation of a variety of functional quinones that allow a systematic modification of the electronic and steric structures.

Assembly of supposedly essential components via covalent linkage is a popular methodology of biomimetic chemistry for biological active sites. Examples other than the porphyrin–quinone systems include a variety of enzyme models,[28] porphyrin–flavin derivatives as models of flavoprotein heme-reductases,[29] and face-to-face bisporphyrins[30] as models of the special-pair chlorophyll dimer in photosynthesis.[31] The present results suggest that well-designed multipoint interactions, especially hydrogen bonding, provide a new, general strategy for the construction of such biologically significant structures[5] or functional molecular assemblies[32] in general. The ultimate goal of the present work is to construct a photosynthesis-mimetic molecular device for efficient charge separation by using functional quinone derivatives. Further work is now under way along this work.

Conclusions

The present host–guest complexation provides a synthetically very simple route to a great variety of face-to-face porphyrin–quinone architectures. The two-point hydrogen bonding gives rise to a sizable selectivity for *p*-quinones as guests. The stability of a resulting adduct is governed not only by the strength of hydrogen bonds involved but also by the porphyrin–quinone interaction of the electrostatic or charge-transfer type. Thus, *both* electron-donating and electron-withdrawing substituents in a guest quinone promote host–guest complexation. The methoxy substituent, however, depresses it for steric reasons. The enforced proximity of the porphyrin and quinone rings in the adducts results in their significant π–π electronic interaction. In addition, the porphyrin fluorescence of the adducts is completely quenched by an efficient, intracomplex electron transfer from photoexcited host porphyrin to bound quinone. Photoreduction of even electron-rich quinones is readily achieved in this manner. Multipoint interaction, especially hydrogen bonding, is a general strategy applicable to molecular-recognition-directed functional assembly of complicated organic molecules.

(26) Stern, O.; Volmer, M. *Phys. Z.* **1919**, *20*, 183.

(27) The Benesi–Hildebrand equation is expressed by $1/\Delta I_{obsd} = 1/\Delta I_{comp} + (1/K)(1/\Delta I_{comp})(1/[\text{quinone}])$ where $\Delta I_{obsd} = I_0 - I_{obsd}$ and $\Delta I_{comp} = I_0 - I_{comp}$. The binding constant ($K$) and the fluorescence property of the complex (I_{comp}, which turned out to be nearly zero) were obtained from the slope and intercept of the plots of $1/\Delta I_{obsd}$ against [quinone].

(28) Reviews: (a) Breslow, R. *Acc. Chem. Res.* **1980**, *13*, 170. (b) Tabushi, I. *Ibid.* **1982**, *15*, 66. (c) Diederich, F. *Angew. Chem., Int. Ed. Engl.* **1988**, *27*, 362.

(29) Takeda, J.; Ohta, S.; Hirobe, M. *J. Am. Chem. Soc.* **1987**, *109*, 7677.

(30) (a) Ogoshi, H.; Sugimoto, H.; Yoshida, Z. *Tetrahedron Lett.* **1977**, *18*, 169. (b) Collman, J. P.; Denisevich, P.; Konai, Y.; Marrocco, M.; Koval, C.; Anson, F. C. *J. Am. Chem. Soc.* **1980**, *102*, 6027. (c) Liu, H. Y.; Weaver, M.; Wang, C. B.; Chang, C. K. *J. Electrochem.* **1983**, *145*, 439.

(31) Wasielewski, M. R.; Svec, W. A.; Cope, B. T. *J. Am. Chem. Soc.* **1978**, *100*, 196.

(32) (a) Lehn, J.-M. *Angew. Chem., Int. Ed. Engl.* **1988**, *27*, 89. (b) Lehn, J.-M. *Ibid.* **1990**, *29*, 1304.

Experimental Section

General Procedure. ^{1}H NMR spectra at 270 MHz were taken for thermostated (within ±0.3 °C) $CDCl_3$ solutions of host **1**, **2**, or **3** ($\sim 5 \times 10^{-3}$ M) on a JEOL-GX 270 spectrometer. The OH proton resonances were identified by deuteriation. IR spectra were obtained for dry $CHCl_3$ solutions of **1** ($\sim 5 \times 10^{-3}$ M) at room temperature by using a JASCO IR-810 spectrophotometer. Electronic spectra were recorded for dry $CHCl_3$ solutions of **1** ($\sim 1 \times 10^{-4}$ M) maintained at 25.0 ± 0.1 °C with a Hitachi 320 spectrophotometer. Fluorescence spectra were taken on a Hitachi F-4000 fluorescence spectrophotometer for degassed solutions of **1** or **4** ($\sim 1 \times 10^{-5}$ M) in benzene (fluorescence grade) at 25.0 ± 0.1 or 11 ± 0.1 °C upon excitation at 544 nm; the fluorescence intensities at 633 nm (for **1**) or 634 nm (for **4**) were measured. Sample preparations were carried out in a dark room. The one-electron redox potential of tetramethoxybenzoquinone (**14**) in acetonitrile was determined by cyclic voltammetry using a Yanagimoto P-1100 polarographic analyzer.[15] Porphyrin derivatives **1**, **2**, and **4** were prepared as described.[33] Quinones and references **5**–**20** except for **14** were commercial products of the highest grades; tetramethoxybenzoquinone (**14**) was obtained in a practically quantitative yield by the reaction of chloranil (**6**) and methanol containing KF and purified by recrystallization from methanol.[34]

Binding Constants. The ^{1}H NMR spectra were taken for a series of solutions containing host **1** at a fixed concentration and varying concentrations of a guest, and the changes in the chemical shifts of the OH groups of **1** were followed. The guests were classified into three categories depending on their affinities to **1** and solubilities in $CDCl_3$: (1) high-affinity and high-solubility guests such as **5**, **10**–**12**, and **15**, (2) high-affinity and low-solubility guests such as **6**–**9** and **17**, and (3) low-affinity and high-solubility guests such as **13**, **14**, **16**, **18**–**20**. For category 1, saturation binding ($\Delta\delta_{comp}$) was readily attained at higher concentrations of guest[35] so that the concentrations of free **1**, free guest, and complex at lower guest concentrations were directly evaluated from $\Delta\delta_{obsd}$. The binding constants were determined from the equation K = [complex]/[**1**][guest]. For categories 3 and 2, the binding constants were obtained by the Benesi-Hildebrand analysis and the Lang's modification thereof, respectively, of the titration data. Similarly were obtained the binding constants for reference hosts **2** and **3** by either the Benesi-Hildebrand or the Lang's method. The concentrations of guests and the temperature ranges were chosen so as to allow a 20–80% range of complexation of host, taking solubilities of guests into account.

UV/visible titration of host **1** with selected quinones was also carried out. The absorbance change at λ_{max} of free **1** (510, 545, 576, or 628 nm) upon addition of a quinone was analyzed according to Benesi-Hildebrand. The binding constants obtained by analysis of the absorbance data at different λ_{max}'s were consistent with each other within 10%.

Acknowledgment. This work was supported by a Grant-in-Aid for Scientific Research on Priority Areas (No. 02230212) from the Ministry of Education, Science, and Culture of the Japanese Government. We are grateful to Dr. Shun-ichi Fukuzumi (Osaka University) for providing us with the redox potential data of quinones. We are also grateful to Dr. Yoshiteru Sakata (Osaka University) for helpful discussion.

(33) (a) Ogoshi, H.; Saita, K.; Sakurai, K.; Watanabe, T.; Toi, H.; Aoyama, Y.; Okamoto, Y. *Tetrahedron Lett.* **1986**, *27*, 6365. (b) Aoyama, Y.; Yamagishi, A.; Tanaka, Y.; Toi, H.; Ogoshi, H. *J. Am. Chem. Soc.* **1987**, *109*, 4735.

(34) Cf. ref 21a.

(35) The $\Delta\delta_{comp}$ value for 1,4-naphthoquinone (**15**) could not be determined experimentally because of overlap of the OH proton resonance of host **1** with the aromatic proton resonance of **15** in a large excess amount. The binding constant for **15** was therefore obtained by the Lang's method.

Photolytic and Solvolytic Reactions of β-[*o*-(Aryloxy)phenyl]vinyl Bromides. Intramolecular Arylation of Vinyl Cations into Dibenzoxepins

Tsugio Kitamura,* Shinjiro Kobayashi, Hiroshi Taniguchi,* and Kenji Hori†

Contribution from the Department of Applied Chemistry, Faculty of Engineering, Kyushu University 36, Hakozaki, Fukuoka 812, Japan, and Department of Chemistry, Faculty of Liberal Arts, Yamaguchi University, Yamaguchi 753, Japan. *Received February 27, 1991*

Abstract: Photolysis of β-[*o*-(aryloxy)phenyl]vinyl bromides, i.e., 2-[*o*-(aryloxy)phenyl]-1-bromo-1,2-diphenylethenes **5**, in dichloromethane gave dibenz[*b*,*f*]oxepins **6** quantitatively. Similar photolysis of vinyl bromides **5** in a mixed solvent of methanol and dichloromethane afforded methanol-incorporated products **7** together with the major dibenz[*b*,*f*]oxepins **6**. Solvolysis of β-[*o*-(*p*-tolyloxy)phenyl]vinyl bromide **5a** in 60% EtOH at 160 °C and acetolysis of β-[*o*-(aryloxy)phenyl]vinyl bromides **5a** and **5c** with silver acetate gave the same dibenz[*b*,*f*]oxepins **6a** and **6c**, respectively. The formation of dibenz[*b*,*f*]oxepins **6** via arylvinyl cations **9** is discussed.

Vinyl cations are recognized as intermediates in organic reactions,[1] especially in solvolytic reactions, where much interest has been paid to the mechanistic aspects. Some approaches to organic synthesis using vinyl cations are valuable, but must overcome several limitations for generating vinyl cations.[1] If these limitations are removed, the method using vinyl cations provides a direct vinylation of substrates. When the vinyl cations possess heteroatoms in the suitable position, this method is useful in the formation of heterocycles. Several studies on the reactivity of the vinyl cations containing heteroatoms have been conducted so far. Modena and co-workers[2] studied vinyl cations having heteroatoms in the β position and found formation of thiirenium ion **1**[2h-m] and

Scheme I

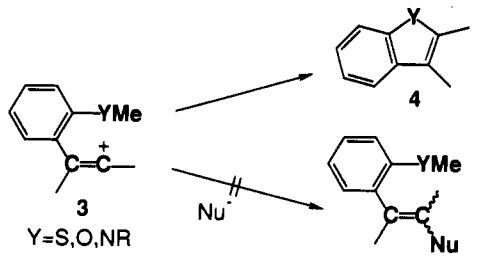

5-membered heterocycles **2** (benzothiophenes,[2a-c] benzofurans,[2f] and indoles[2g]).

† Yamaguchi University.

0002-7863/91/1513-6240$02.50/0